Dynamic dielectric properties of isotactic polypropylene-g-maleic anhydride crosslinked by capped-end polyether diamine and filled with native or functionalized nano-graphite particles

F. Agrebi, A. Letoffé, A. Kallel, I. Royaud, Z. Ayadi, M. Ponçot, Stéphane Cuynet, Sébastien Fontana

Metadata of the article that will be visualized in OnlineFirst

ArticleTitle	Dynamic dielectric properties of isotactic polypropylene-g-maleic anhydride crosslinked by capped-end polyether diamine and filled with native or functionalized nano-graphite particles	
Article Sub-Title		
Article CopyRight	The Author(s), under exclusive licence to Springer-Verlag GmbH Germany, part of Springer Nature (This will be the copyright line in the final PDF)	
Journal Name	Polymer Bulletin	
Corresponding Author	FamilyName	**Royaud**
	Particle	
	Given Name	**I.**
	Suffix	
	Division	CNRS, IJL
	Organization	Université de Lorraine
	Address	54000, Nancy, France
	Division	
	Organization	Université de Lorraine, CNRS, LabEx "DAMAS"
	Address	57000, Metz, France
	Phone	
	Fax	
	Email	Isabelle.royaud@univ-lorraine.fr
	URL	
	ORCID	http://orcid.org/0000-0001-5469-2995
Author	FamilyName	**Agrebi**
	Particle	
	Given Name	**F.**
	Suffix	
	Division	Faculty of Sciences of Sfax, LaMaCoP
	Organization	University of Sfax
	Address	3018, Sfax, BP, Tunisia
	Phone	
	Fax	
	Email	
	URL	
	ORCID	
Author	FamilyName	**Letoffe**
	Particle	
	Given Name	**A.**
	Suffix	
	Division	CNRS, IJL
	Organization	Université de Lorraine
	Address	54000, Nancy, France
	Division	
	Organization	Université de Lorraine, CNRS, LabEx "DAMAS"
	Address	57000, Metz, France
	Phone	
	Fax	
	Email	
	URL	
	ORCID	

Author	FamilyName	**Kallel**
	Particle	
	Given Name	**A.**
	Suffix	
	Division	Faculty of Sciences of Sfax, LaMaCoP
	Organization	University of Sfax
	Address	3018, Sfax, BP, Tunisia
	Phone	
	Fax	
	Email	
	URL	
	ORCID	
Author	FamilyName	**Ayadi**
	Particle	
	Given Name	**Z.**
	Suffix	
	Division	CNRS, IJL
	Organization	Université de Lorraine
	Address	54000, Nancy, France
	Phone	
	Fax	
	Email	
	URL	
	ORCID	
Author	FamilyName	**Ponçot**
	Particle	
	Given Name	**M.**
	Suffix	
	Division	CNRS, IJL
	Organization	Université de Lorraine
	Address	54000, Nancy, France
	Division	
	Organization	Université de Lorraine, CNRS, LabEx "DAMAS"
	Address	57000, Metz, France
	Phone	
	Fax	
	Email	
	URL	
	ORCID	
Author	FamilyName	**Cuynet**
	Particle	
	Given Name	**S.**
	Suffix	
	Division	CNRS, IJL
	Organization	Université de Lorraine
	Address	54000, Nancy, France
	Phone	
	Fax	
	Email	
	URL	
	ORCID	

Author	FamilyName	**Fontana**
	Particle	
	Given Name	**S.**
	Suffix	
	Division	CNRS, IJL
	Organization	Université de Lorraine
	Address	54000, Nancy, France
	Phone	
	Fax	
	Email	
	URL	
	ORCID	

Schedule	Received	2 Jan 2022
	Revised	11 Feb 2022
	Accepted	22 Feb 2022

Abstract	Dynamic dielectric properties of an isotactic polypropylene matrix grafted with maleic anhydride (CA 100) and then crosslinked by polyether amine molecules and reinforced with different weight percentages of graphite nanoplatelets (GNPs), KNG180, were studied for the first time and compared to those obtained by DMA (Dynamic Mechanical Analysis). The main objective of this work was to investigate the reinforcement effect of GNPs focusing on the GNPs/matrix interfacial adhesion using dynamic dielectric relaxation spectroscopy in the frequency range from 0.1 Hz to 1 MHz and temperature range from 20 to 140 °C. The obtained interfacial polarization increments $\Delta\varepsilon_{MWS}$ from MWS (Maxwell Wagners Sillars) relaxation showed a threshold value of 3% in weight of KNG180. This analysis suggests that interfacial compatibility between matrix and fillers in the case of nanocomposite KNG180 3 wt% is higher than those of other nanocomposites. A new plasma treatment was used to modify graphite nano-fillers to produce different types of nanocomposites. The 5 wt% plasma treated graphite nanocomposite shows a good dispersion of the nano-fillers but also a high value of $\Delta\varepsilon_{MWS}$, which is an indication of high graphite/graphite interaction. This evolution could show that this material can be close to the formation of an electrical percolation network.

Keywords (separated by '-')	Isotactic polypropylene - Graphite nanosheets - Dynamic dielectric properties
Footnote Information	

Journal : SmallExtended 289	Article No : 4171	Pages : 20	MS Code : 4171	Dispatch : 20-3-2022

Polymer Bulletin
https://doi.org/10.1007/s00289-022-04171-9

ORIGINAL PAPER

Dynamic dielectric properties of isotactic polypropylene-g-maleic anhydride crosslinked by capped-end polyether diamine and filled with native or functionalized nano-graphite particles

F. Agrebi[2] · A. Letoffe[1,3] · A. Kallel[2] · I. Royaud[1,3] · Z. Ayadi[1] · M. Ponçot[1,3] · S. Cuynet[1] · S. Fontana[1]

Received: 2 January 2022 / Revised: 11 February 2022 / Accepted: 22 February 2022

Abstract

Dynamic dielectric properties of an isotactic polypropylene matrix grafted with maleic anhydride (CA 100) and then crosslinked by polyether amine molecules and reinforced with different weight percentages of graphite nanoplatelets (GNPs), KNG180, were studied for the first time and compared to those obtained by DMA (Dynamic Mechanical Analysis). The main objective of this work was to investigate the reinforcement effect of GNPs focusing on the GNPs/matrix interfacial adhesion using dynamic dielectric relaxation spectroscopy in the frequency range from 0.1 Hz to 1 MHz and temperature range from 20 to 140 °C. The obtained interfacial polarization increments $\Delta\varepsilon_{MWS}$ from MWS (Maxwell Wagners Sillars) relaxation showed a threshold value of 3% in weight of KNG180. This analysis suggests that interfacial compatibility between matrix and fillers in the case of nanocomposite KNG180 3 wt% is higher than those of other nanocomposites. A new plasma treatment was used to modify graphite nano-fillers to produce different types of nanocomposites. The 5 wt% plasma treated graphite nanocomposite shows a good dispersion of the nano-fillers but also a high value of $\Delta\varepsilon_{MWS}$, which is an indication of high graphite/graphite interaction. This evolution could show that this material can be close to the formation of an electrical percolation network.

Keywords Isotactic polypropylene · Graphite nanosheets · Dynamic dielectric properties

✉ I. Royaud
Isabelle.royaud@univ-lorraine.fr

[1] CNRS, IJL, Université de Lorraine, 54000 Nancy, France

[2] Faculty of Sciences of Sfax, LaMaCoP, University of Sfax, 3018 Sfax, BP, Tunisia

[3] Université de Lorraine, CNRS, LabEx "DAMAS", 57000 Metz, France

Journal : SmallExtended 289	Article No : 4171	Pages : 20	MS Code : 4171	Dispatch : 20-3-2022

Introduction

Polypropylene (PP) is a well-known semi-crystalline thermoplastic polymer which has been widely applied in many fields. Along the past two decades, PP has been reinforced with several fibers to enhance its mechanical and physical properties. Lately, PP/Graphite and PP/graphene composites have attracted great research interest, because mechanical as well as physical properties (thermal conductivity, electrical conductivity, barrier property, etc.) can be simultaneously improved to fulfill the requirements of many practical applications [1]. The isotactic polypropylene or iPP was mainly chosen for its mechanical properties with regards to the nanocomposite conception. It is a well-known material for its properties and generally used in a lot of industrial application. The main advantage of this nanocomposite is its capability to be used in different industrial application and specifically in the automotive industry, the polymer/metal composite to enlightened the structure. Composites based on isotactic polypropylene anhydride (iPP-g-MAH) crosslinked by the use of polyetheramine molecules [2] were studied in this work as a matrix reinforced with graphite nanosheets (GNPs), KNG 180. Since, the use of maleic anhydride (MAH) is one of the most common ways in the reactive blending to improve the interfacial adhesion in immiscible polymer blends, particles and fibers filled polymer matrix and multi-layered multi-material's composites [3].

The GNPs used as nano-reinforcing phase were characterized and successfully dispersed into iPP-g-MAH matrix to produce iPP-g-MAH/GNPs nanocomposites. In polymers and composite polymer materials, interfacial polarization is almost present due to the existence of heterogeneities (multiphase systems, semi crystalline polymers, fillers, impurities). Many techniques have been used to explore the interface. Among these techniques, Broadband Dielectric spectroscopy (BDS) is one of the most powerful methods providing a direct experimental access to a variety of physical phenomena taking place at different length and time-scale, such as molecular fluctuation, charge transport processes in the bulk and at the interfaces [4]. That is why in this paper, the effects of the incorporated GNPs with loading of various content (1 wt%, 3 wt%, 5 wt% and 10 wt %) on the dielectric properties of iPP-g-MAH matrix were investigated using this technique [5].

Experimental

Materials

The polypropylene grafted maleic anhydride used in this work is the Orevac® CA 100 from Arkema. This isotactic polypropylene is grafted with 1 wt% of maleic anhydride. The maleic anhydride grafting to the iPP plays an important role in two ways: First, it is well known in the literature that adding MAH to a polymer such as the polypropylene can help the dispersion of a carbon–nano-filler such

Journal : SmallExtended 289	Article No : 4171	Pages : 20	MS Code : 4171	Dispatch : 20-3-2022

as graphite when there is poor compatibility between the filler and the matrix. PP-g-MAH was used as the nanocomposite matrix because of this reason. The main problem comes from the poor mechanical behaviour of such matrix (it is brittle). Thus, a crosslinked reaction that used diamine molecule and the graft MAH was developed to improve the polymer mechanical behaviour and obtain a ductile matrix. In this situation, the MAH helps for the homogeneous dispersion of the filler and for the crosslinking reaction used to improve the mechanical properties. In the context of automotive industry and polymer/metal composite, it is the adhesion then the crosslinking and then an help to the dispersion of the fillers which is aimed (duality functionalization and conduction from percolation of the matrix).

The technical specification sheet provides by Arkema indicated a yield strength of 22 MPa and an elongation at break of 12% [6]. The CA 100 average molecular weight is estimated at $\overline{M_n}$=25,000 g mol^{-1}[8, 9].

The crosslinking agent used is the Jeffamine® THF 100 by huntsman [10]. It is a capped-end triblock polyether diamine (H_2N–PO_2–TMO_9–PO_3–NH_2) and used as received. It possesses a molecular weight of 1000 g mol^{-1}.

Two graphites were used in this work. The first one is a GNP from Knano (Xianen, China) under the reference KNG 180. It presents a high carbon content (> 99.5 wt%), a diameter between 8 and 100 µm and a thickness inferior to 100 nm (supplier data). The second one is a KNG 180 treated by a new plasma treatment developed for the exfoliation and functionalization of the graphite. The characterization of those functionalized nano-fillers was already performed in a previous work [11].

Material's preparation

The crosslinked material was produced with the method described in a previous article [2, 6, 7]. The Jeffamine® THF 100 by Huntsman was used to crosslink the CA 100 by reactive extrusion as described in our previous work [2]. The matrix was crosslinked with an amine:MAH molar ratio of 1:1. This configuration gives the best mechanical properties. This material is noted CA 100 THF 100 1:1. This matrix is used as reference.

The nanocomposites elaboration was performed at LRGP Laboratory (CNRS-University of Lorraine, Nancy, France), with a 10 mm barrel extruder (Twinscrew Benthop Compounding Line from Rondol Technology LdT), with a L:D ratio of 40:1. The rotation speed was fixed at a specific value of 20 rpm. The process is a variation of the process use for the crosslinked matrix [2, 6, 7]. Figure 1 shows the screw and temperature profile of the extruder.

A nanocomposite which can be processed at large scale using conventional method for polymer processing had to be looked for (i.e., without any particular investment/development). In previous test, the carbon nano-fillers were added early in the extrusion process but it was difficult to produce a homogeneous material due to the behaviour of the filler. By introducing the fillers after the polymer (CA 100) was completely mixed with the crosslinking agent (THF 100) in

Journal : SmallExtended 289	Article No : 4171	Pages : 20	MS Code : 4171	Dispatch : 20-3-2022

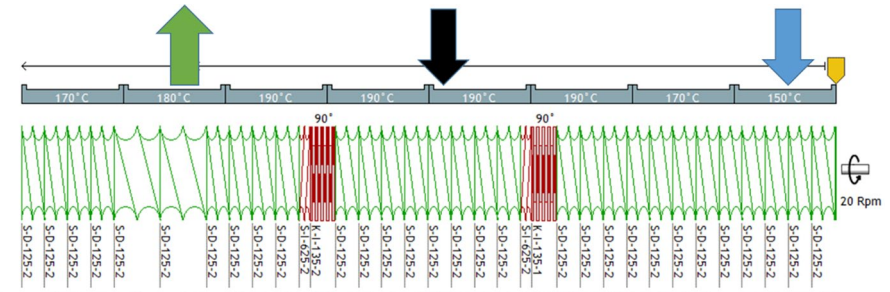

Fig. 1 Temperature and screw profile used for the nanocomposite's elaboration. The mixing areas are in red and the conveyor element in green. The arrows indicate the introduction of the CA 100 (blue), of the crosslink agent/carbon nano-fillers (black) and the solvent extraction by vacuum pomp (green)

a solvent (mesitylene), a better control of the filler concentration and dispersion was obtained [2]. The low screw rotation was imposed by the crosslinked reaction used in this work to produce the composite. After the introduction of the crosslinking agent in the melted CA 100, a minimum of 10 min is necessary to complete the chemical reaction. The screw rotation was calculated to obtain the optimal residence time. The CA 100 was introduced with a mass flow of 1.1 g min^{-1}. The nano-fillers (KNG-180 and KNG-180 plasma treated) and the crosslinking agent (THF 100) were mixed together with mesitylene to obtain a low viscosity liquid that can be injected. The filler dispersion was obtained by a sonic bath. The mixture was injected into the extruder barrel between the two mixing areas, the mass flow rate was adapted to rich the targeted molar ratios NH_2:MAH and nano-filler concentration. Two screw elements with large thread were added at the end of the extruder to help the mesitylene evaporation. A vacuum pump connected to the extruder barrel and a cold trap with liquid nitrogen performed its extraction. The complete extraction of mesitylene was confirmed by FTIR spectroscopy. Two types of nanocomposite were produced. The first one with the unmodified KNG 180, with an amine:MAH molar ratio of 1:1 and a carbon concentration of 1, 3, 5 and 10 wt%. The second type was produced with the plasma treated fillers, with a concentration of 1, 3 and 5 wt%.

The crosslinked matrix and the nanocomposites were shaped into 3 mm plates with injection moulding (Micro 12 cc Injection Moulding Machine/DSM Xplore). The filler concentration was confirmed by TGA analysis.

Experimental procedure

SEM and TEM microscopy

SEM micrographs were obtained after the samples were broken by cryofracture. The fracture pattern was examined by an environmental Quanta FEG 650 electron microscope from FEI Company. The electrons were accelerated under a tension of 4 kV, under a water vapor pressure of 100 Pa.

Journal : SmallExtended 289	Article No : 4171	Pages : 20	MS Code : 4171	Dispatch : 20-3-2022

Transmission electron microscopy, or TEM, was performed on an ARM-200F apparatus at an operating voltage of 200 kV. Samples were dispersed in absolute ethanol by sonication and were deposited on a copper grid and a holey carbon film.

Dynamic dielectric spectroscopy (DDS)

The dynamic dielectric spectroscopy experiments were carried out using a Novocontrol System based on an Alpha Analyzer and a temperature controller (Novocontrol quatro system controller BDS 1330) at the frequency range from 0.1 Hz to 1 MHz and the temperature range from 20 to 140 °C on heating at a rate of 5 °C/min. The sample was fixed between two additional external electrodes of 20 mm in diameter in the sample holder and placed in a cryostat. The measured dielectric permittivity data were collected and evaluated by WinDETA impedance analysis software. According to the planar capacitor rule, the complex dielectric function for the polymer is expressed as [12–16]

$$\varepsilon^*(\omega) = \varepsilon'(\omega) - j\varepsilon''(\omega)\,(j \text{ is the square root of } -1), \tag{1}$$

where ε' and ε'' are the real and imaginary parts of the complex permittivity.

The AC conductivity of all samples has been calculated from the dielectric losses according to the relation:

$$\sigma^*(\omega) = j\varepsilon_0\omega\varepsilon^*(\omega) = j\varepsilon_0\omega\left(\varepsilon' - j\varepsilon''\right) = \varepsilon_0\omega\varepsilon'' + j\varepsilon_0\omega\varepsilon'. \tag{2}$$

The real part of $\sigma^*(\omega)$ is given by

$$\sigma_{AC}(\omega) = \varepsilon_0\omega\varepsilon''(\omega), \tag{3}$$

where ε_0 is the dielectric permittivity in vacuum (8.85×10^{-12} F·m^{-1}) and ω is the angular frequency.

The complex dielectric permittivity can be written as a function of angular frequency ($\omega = 2\pi f$) in accordance with numerous possible relaxation processes caused by the mobility of different dipoles and charges in the systems and described by the Havriliak–Negami (HN) [17, 18] according to the following equation (4):

$$\varepsilon^*(\omega) = \varepsilon_\infty + \sum_i \left[\frac{\Delta\varepsilon_i}{\left(1 + \left(j\omega\tau_{\mathrm{HN}i}\right)^{\alpha_i}\right)^{\beta_i}}\right] - j\frac{\sigma_{dc}}{\varepsilon_0\omega}. \tag{4}$$

The parameters α_i and β_i [$0 < \alpha_i$; $\alpha_i\beta_i \leq 1$] define the symmetrical and asymmetrical broadening of the distribution of relaxation times, respectively. $\tau_{\mathrm{HN}i}$ the characteristic relaxation time and $\Delta\varepsilon_i$ is the relaxation strength values. $\left(-j\sigma_{dc}/\varepsilon_0\omega\right)$ is the dc conductivity term. The index i represents the different relaxations involved in dielectric spectra.

Two kinds of dielectric experiments were conducted: isothermal runs with fixed temperatures and scanning frequencies and isochronal runs with fixed frequencies and varying temperature. In this work, our attention is focused on isothermal runs.

Journal : SmallExtended 289	Article No : 4171	Pages : 20	MS Code : 4171	Dispatch : 20-3-2022

Dynamic mechanical analysis (DMA)

The dynamic mechanical properties of the materials were determined using DMA 242C manufactured by Netzsch. Rectangular bar shaped samples of dimension $20 \times 4 \times 3$ mm^3 were machined out. The complex modulus measurement were performed in three points bending mode at three different frequencies at 1 Hz from – 80 °C to 110 °C and at a constant heating rate of 2 °C min^{-1}.

Results and discussion

Scanning and transmission electronic microscopy analysis

SEM and TEM microscopy were performed to analyse the filler dispersion inside the different nanocomposites. Figure 2 shows TEM and SEM micrographs for the CA 100 THF 100 1:1 with 1 wt% of KNG 180.

For those materials, a good dispersion of the nano-fillers inside the polymer matrix was observed with no aggregation of the graphite flakes. No debonding between the graphite and the polymer was observed even after the sample preparation (cryofracturation). This indicates a good compatibility between the polymer and the graphite. This was not expected due to the poor interaction between the polypropylene and the graphite. The polyether diamine used to crosslink the material must play an important role in the improvement of this compatibility.

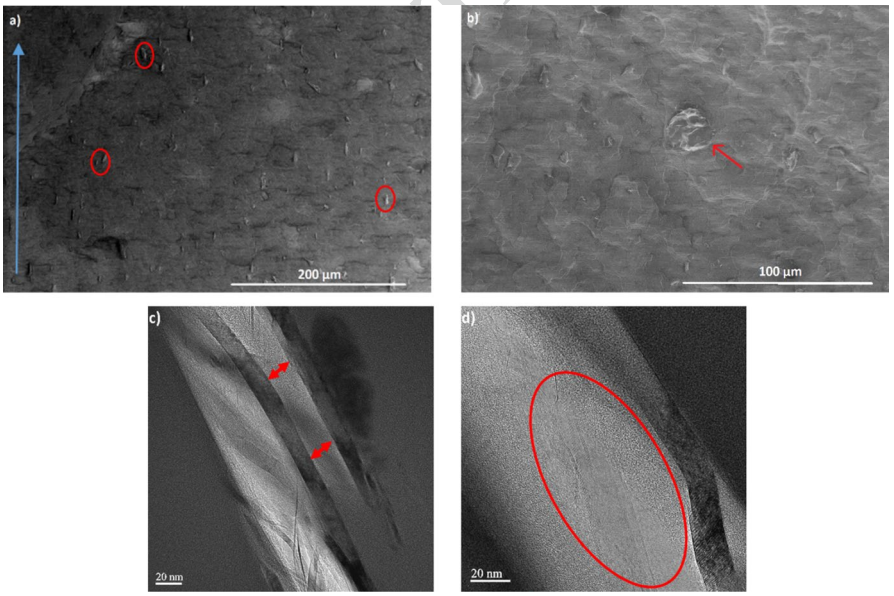

Fig. 2 SEM (**a**, **b**) and TEM (**c**, **d**) micrographs of the CA 100 THF 100 1:1 KNG-180 1 wt% nanocomposites. In **a**, the blue arrow indicate the injection flow direction

Journal : SmallExtended 289	Article No : 4171	Pages : 20	MS Code : 4171	Dispatch : 20-3-2022

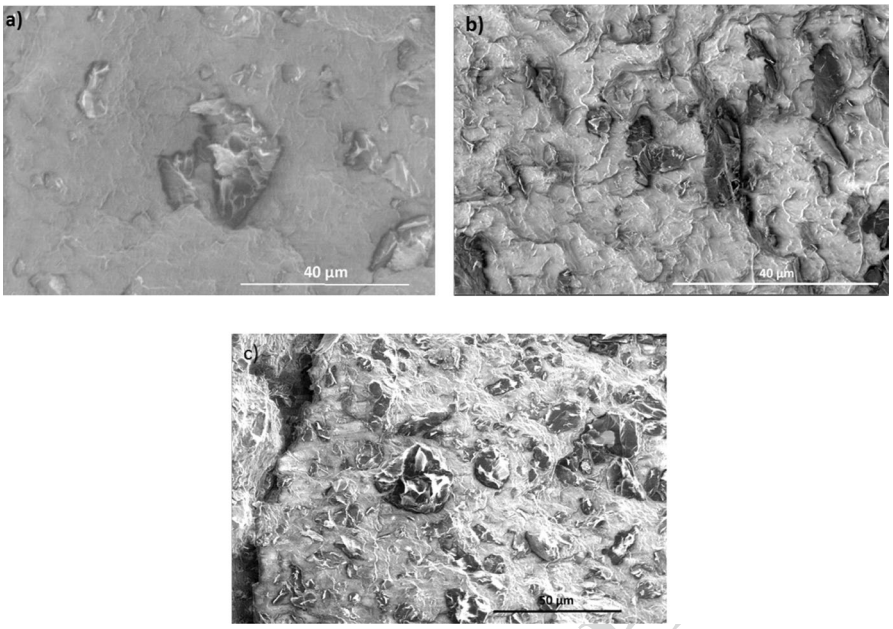

Fig. 3 SEM micrograph of the CA 100 THF 100 1:1 KNG-180 nanocomposites at 3 wt% (**a**), 5 wt% (**b**) and 10 wt% (**c**)

Figure 3 exhibits SEM micrograph for the CA 100 THF 100 1:1 filled with KNG-180 at 3, 5 and 10 wt%. The nanocomposite filled at 3 wt% of KNG-180 shows a good dispersion of the nano-filler inside the matrix. On the contrary, the nanocomposite at 5 wt% shows the formation of small aggregates, which are more important at 10 wt%. The dispersion quality and polymer/carbon compatibility seem to fall for the concentration above 3 wt%.

Figure 4 exhibits SEM micrographs of the three nanocomposites filled with plasma treated KNG-180. Like for the nanocomposites filled with untreated KNG-180, the treated graphite seems to present a high adhesion to the polymer matrix, with no debonding. No aggregation can be observed for the nanocomposite filled at 5 wt%. This is an important difference compared with the untreated KNG-180 which implied that the functionalization of the graphite improves the dispersion of the nano-fillers, hence the good polymer/carbon compatibility. This behavior could be investigated by dynamic dielectric spectroscopy.

Figures 5 and 6 depict the comparison of the DMA signals recorded for the loss factor at 1 Hz as a function of temperature for untreated and plasma treated nanocomposites, respectively. All nanocomposites show the polypropylene relaxations α, β and γ [19].

The γ-relaxation around − 40 °C related to the methyl groups motion, show low amplitude variation with the filler concentration. No significate variation can be observed with the type of filler or the carbon concentration.

Journal : SmallExtended 289	Article No : 4171	Pages : 20	MS Code : 4171	Dispatch : 20-3-2022

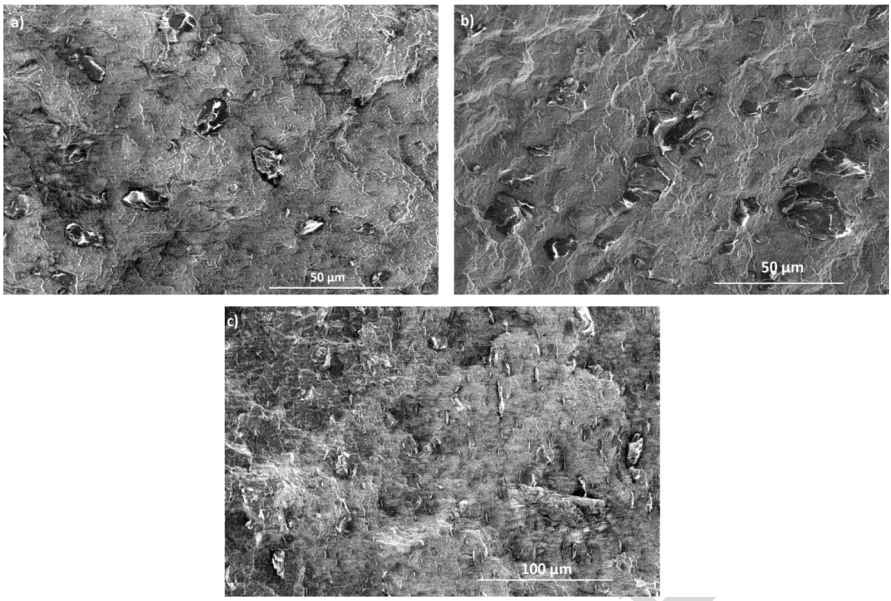

Fig. 4 SEM micrography of the CA 100 THF 100 1:1 KNG-180 plasma treated nanocomposites at 1 wt% (**a**), 3 wt% (**b**) and 5 wt% (**c**)

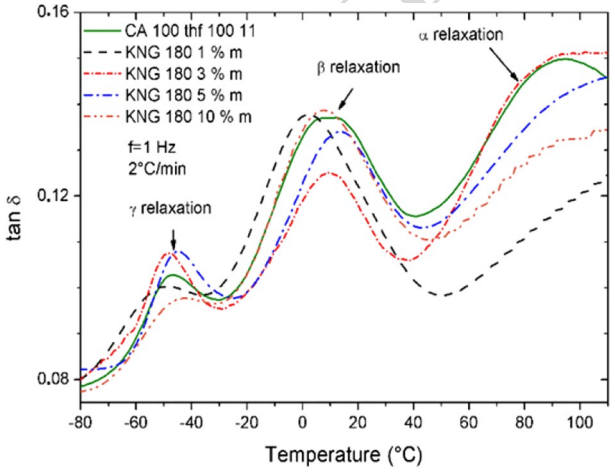

Fig. 5 Evolution of the loss factor of the CA 100 THF 100 1:1 filled with the unmodified KNG-180 between 1 and 10 wt%

The β-relaxation, associated to the glass transition of the polypropylene, presents different amplitudes but also important variation of temperature. The initial crosslinked material, the CA 100 THF 100 1:1 exhibits a β-relaxation associated to the glass transition at 11 °C. The nanocomposite filled with 1wt% of KNG-180

Journal : SmallExtended 289	Article No : 4171	Pages : 20	MS Code : 4171	Dispatch : 20-3-2022

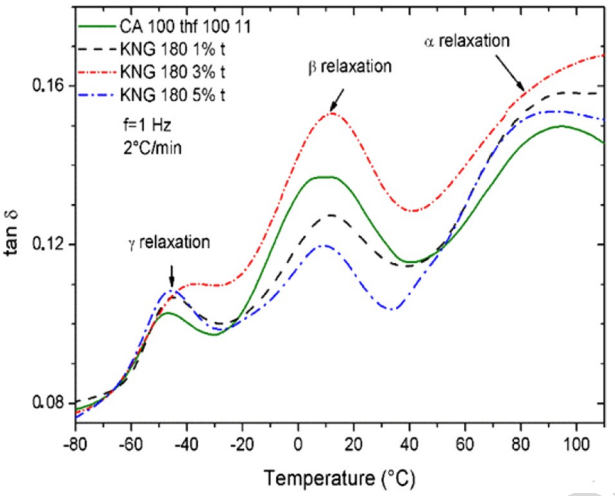

Fig. 6 Evolution of the loss factor of the CA 100 THF 100 1:1 filled with the KNG-180 plasma treated between 1 and 5 wt%

present a fall of the glass transition temperature to 1 °C. This temperature rises with the filler content with a maximum of 14 °C at 5 wt%, and falls to 10 °C again at 10 wt%. The nano-fillers seem to affect the amorphous chains mobility depending on the carbon concentration. The first fall could be explained by a degradation of the crosslinking network by the carbon filler. On the opposite, the rise observed between 1 wt% and 5 wt% of carbon filler shows that the KNG-180 impacts the polypropylene macromolecular chains mobility. These results are in with the literature on the nanocomposite elaboration [20, 21]. The final fall, between 5 and 10 wt%, can be linked to the formation of the aggregate of the filler inside the matrix and the dispersion then the degradation. On the opposite, the nanocomposite filled with the KNG-180 plasma treated shows a small rise of its glass transition temperature, from 12 °C at 1 wt%, to 13 °C at 3 and 5 wt%. This evolution, different from the untreated fillers materials, can be explained by a higher compatibility between the polymer and the filler and a better dispersion as observed by SEM and TEM microscopy.

Finally, the α-relaxation, associated to local motions within the crystalline phase is located around 90 °C for the nanocomposites. The relaxation amplitudes exhibit an important variation that could be explained by the crystalline phase evolution and the possible transcristallinity on the graphite surface.

Dynamic dielectric analysis studies

CA 100 matrix

Figure 7 shows the real and imaginary parts of the complex permittivity versus frequency, for the matrix isotactic polypropylene grafted with maleic anhydride CA 100 THF 100 crosslinked in ratio 1:1 (noted CA 100 THF 100 1:1).

Journal : SmallExtended 289	Article No : 4171	Pages : 20	MS Code : 4171	Dispatch : 20-3-2022

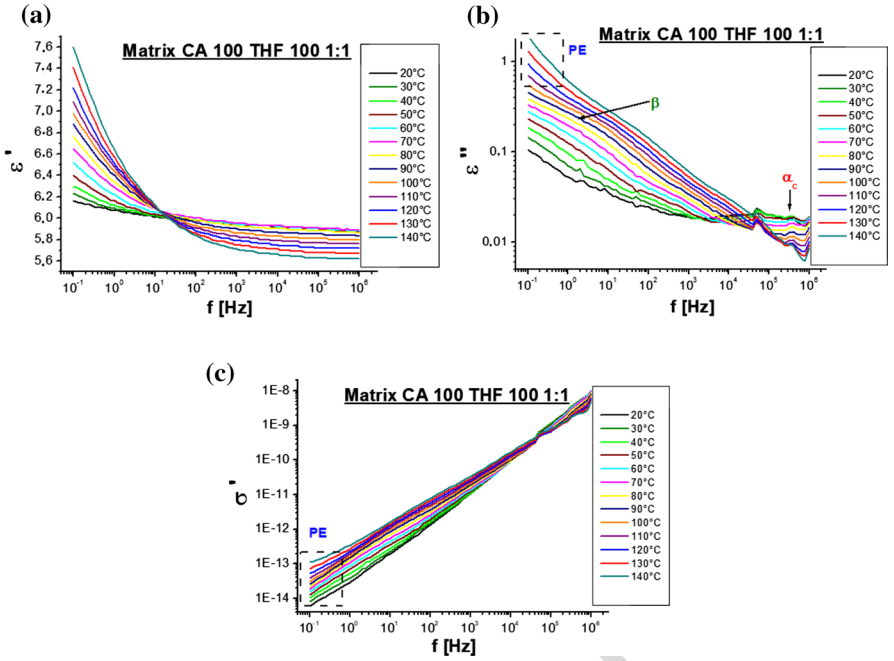

Fig. 7 Frequency dependence of (**a**) ε', (**b**) ε'' and (**c**) σ_{ac} for the matrix CA 100 THF 100 1:1 at the temperature region [20–140 °C]

ε' is related to the number of dipoles which re-orient in the electric field, thus when the temperature is varied, the signal is changing drastically when the different relaxations occur in the material under study (i.e., polypropylene grafted MAH and crosslinked macromolecular chains).

Three relaxation phenomena can be observed. The first one appears between 10^3 Hz and 1 MHz which could be ascribed to the α_c relaxation related to the crystalline phase [22]. The PP grafted with maleic anhydride presented higher crystallinity percentages than did the pure PP. The increase in the percentage of crystallinity was ascribed to the reduction in molecular weight and to the rise of polarity of the grafted samples [23]. The second relaxation process is observed around 10^2 Hz which can be ascribed to the sub-glass transition relaxation (β-relaxation) [24], and is related to the presence of polar maleic anhydride/amide/imide groups present in the polymer [25]. These two relaxations are also observed in DMA analysis [2] (Figs. 5, 6). The third relaxation, the γ relaxation associated with the movements of the methyl groups of the polypropylene chain appears only at lower temperature range (around $-50°C$) and cannot be observed here. Due to the important difference between the two experimental methods, the temperatures and amplitudes associated to the different relaxations shows important variations, and make the comparison difficult. The DMA seem more appropriate to analyses the small variation of the relaxation temperature such as the β-relaxation associated with the glass transition, but the dielectric spectroscopy allow an analysis at high frequency. In addition,

the MWS relaxation localized at the interface between the polymer and the matrix that will be used to describe the nanocomposite cannot be observed by DMA.

No important differences between the electrical or dielectrical property of isotactic, atactic and syndiotactic polypropylene are expected. Some differences can be found in the capacity of the dipoles to re-orient in the electrical filed if the polymer is crystalline (isotactic and syndiotactic) compared to a more amorphous atactic polypropylene but these slight differences would not be seen at the interfaces with the graphite filler when observing the MWS relaxation.

Another special feature, ascribed to the electrode polarization (EP), can be detected from Fig. 7 by a large dispersion of ε' ($\Delta\varepsilon \gg 1$) in low frequency region. Such mechanism is detected again on the variation of the electrical conductivity σ_{ac} versus frequency (see Fig. 7c) by a significant decrease of σ_{ac} in low frequencies below the plateau region which, therefore, tends to be superimposed on the dc bulk conductivity (σ_{dc}) [4].

Nanocomposites with untreated KNG180

The addition of GNPs into CA 100 THF 100 1:1 matrix increases the dielectric losses and generates other relaxation processes, directly related to the fillers, according to Fig. 8.

The crystalline peak α_c is found to be at about the same temperature with a higher intensity and correspondingly larger area. Moreover, an additional process appears at higher temperature and is ascribed to the interfacial polarization known as the Maxwell–Wagner–Sillars (MWS) effect. This relaxation arises from the accumulation of charge carriers at the interfaces between the GNPs and CA 100 THF 100 1:1 matrix deriving a more or less conductive material depending on the nature, size and the volume fraction of the filler.

Table 1 presents the interfacial dielectric increments or polarization intensities $\Delta\varepsilon_{MWS}$, defined by $\Delta\varepsilon_{MWS} = \varepsilon_s - \varepsilon_\infty$ [26, 27] and deduced by fitting curves using the following Havriliak–Negami (HN) function:

$$\varepsilon'' = \sum_i \left[\frac{\Delta\varepsilon_i \sin\beta\varphi}{\left[1 + 2(\omega\tau_{HNi})^{\alpha_i}\cos\left(\alpha_i\frac{\pi}{2}\right) + (\omega\tau_{HNi})^{2\alpha_i}\right]^{\frac{\beta_i}{2}}} \right] + j \times \frac{\sigma_{dc}}{\varepsilon_0\omega}, \tag{5}$$

$$\text{With, } \varphi = \arctan\frac{(\omega\tau)^{\alpha}\sin\left(\alpha\frac{\pi}{2}\right)}{1 + (\omega\tau)^{\alpha}\cos\left(\alpha\frac{\pi}{2}\right)} \text{ and } \tau_{\max,\varepsilon} = \tau_{HN}\left[\frac{\sin\left(\frac{\alpha\beta\pi}{2+2\beta}\right)}{\sin\left(\frac{\alpha\pi}{2+2\beta}\right)}\right]^{\frac{1}{\alpha}}. \tag{6}$$

One example of the fitting procedure with a separation of overlapping relaxation regions via the deconvolution of ε'' at 130 °C and between 0.1 Hz and 10^4 Hz is shown in Fig. 9 for all nanocomposites.

Journal : SmallExtended 289	Article No : 4171	Pages : 20	MS Code : 4171	Dispatch : 20-3-2022

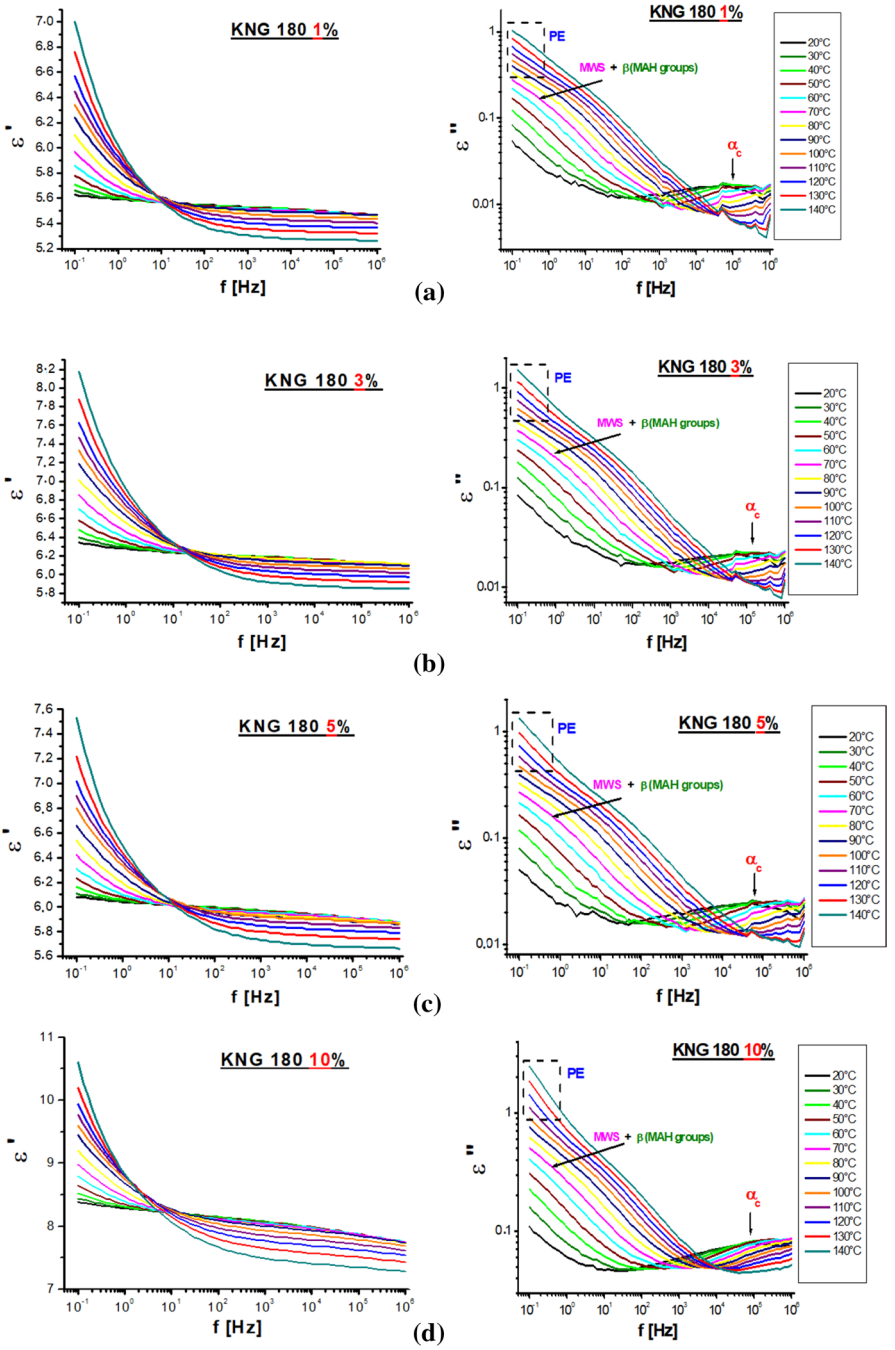

Fig. 8 Frequency dependence of ε' and ε'' for the nanocomposites KNG-180 **a** 1%, **b** 3%, **c** 5% and **d** 10% at the temperature region [20–140 °C]

Table 1 MWS polarization dielectric increments for all unmodified nanocomposites

	$\Delta\varepsilon_{MWS}$ (1801m%)	$\Delta\varepsilon_{MWS}$ (1803m%)	$\Delta\varepsilon_{MWS}$ (1805m%)	$\Delta\varepsilon_{MWS}$ (18010m%)
100 °C	0.24	0.18	0.26	0.27
110 °C	0.27	0.19	0.29	0.32
120 °C	0.28	0.26	0.32	0.35
130 °C	0.35	0.34	0.39	0.42
140 °C	0.40	0.39	0.43	0.54

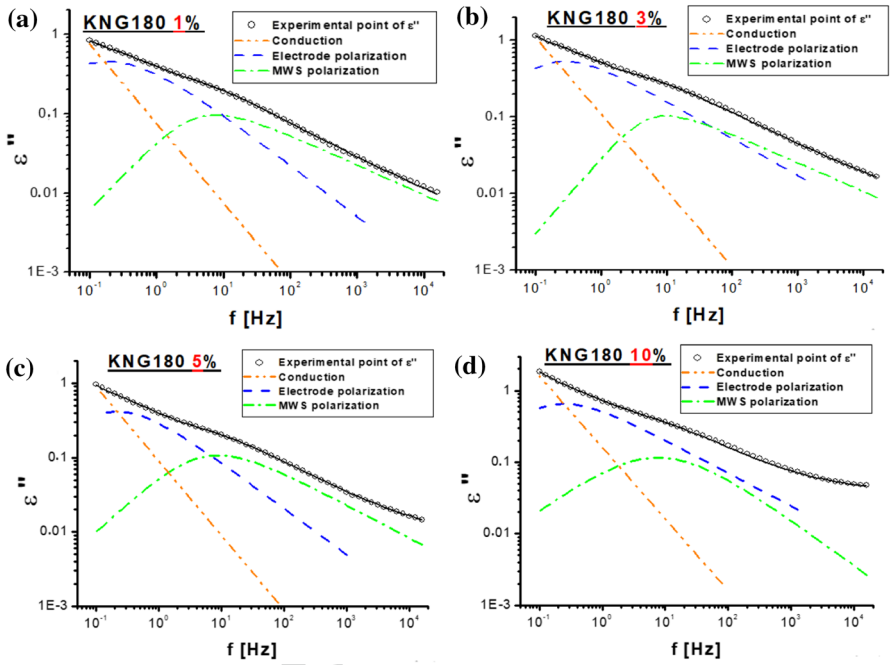

Fig. 9 Imaginary part of ε'' versus frequency for nanocomposites **a** KNG-180 1%, **b** KNG-180 3%, **c** KNG-180 5% and **d** KNG-180 10% at 130 °C and between 0.1 and 10^4 Hz. Solid lines indicate the fit by Havriliak–Negami model (Eq. 4) and dashed lines indicate the deconvolution of ε'' according to different processes

It is clear, from Table 1, that $\Delta\varepsilon_{MWS}$ increased with the temperature. This phenomenon is due to the greatest number of free charges, which can migrate and then block towards the GNPs/CA 100 THF 100 1:1 matrix interfaces. In general, it is noted that a rise in the temperature leads to an increase in the relaxation accompanied with shift of the maximum towards the high frequencies suggesting that the aptitude of the charge carriers to be polarized at the interface is more important at high temperatures [4, 28].

Furthermore, the variation of the interfacial polarization intensities gives us an idea about both types of interactions filler–filler and filler–matrix [29]. As it can be seen, the interfacial polarization intensities $\Delta\varepsilon_{MWS}$ showed a threshold

value of 3% in weight of KNG-180. Variations were explained with attractive and repulsive GNPs–GNPs and GNPs-CA 100 THF 100 1:1 matrix interaction. A decrease in MWS polarization intensity with the increase of the reinforcement (from 1 wt% to 3 wt% of KNG-180) (see Table 1) can be noted. This is explained by a better adhesion between the reinforcement and the matrix indicating a rigidification of the GNPs-CA 100 THF 100 1:1 matrix interfacial region which in turn reduced the ability of dipole to relax. This result is in good agreement with DMA analysis. Incorporating higher KNG-180 content (5 wt% and 10 wt% of GNPs) leads to reduce their mutual distances and interactions between GNPs start to occur, in good coherence with SEM and TEM, which enhances the formation of small aggregates. These interactions become stronger than those of GNPs–matrix (see Fig. 4). In fact, increases in the polarization intensity are interpreted with repulsive interactions between the CA 100 THF 100 1:1 matrix and GNPs. However, decreases in the polarization intensity are explained with high attractive GNPs–GNPs interactions and predominately GNPs–matrix interactions. In this case, the better distribution of the GNPs reduces agglomeration and increases the reinforcement effect of GNPs (see Fig. 10).

In view of that, the properties of polymer nanocomposites largely depend on the dispersion and distribution of nanofillers within the matrix, the filler–polymer compatibility and their interfacial interaction, the nanofiller content should be, therefore, carefully chosen to have better properties. In this case, it can be concluded that the nanocomposite with 3% of GNPs (KNG 180 3%) has the best rigidity given their low value of $\Delta\varepsilon_{MWS}$ compared to other nanocomposites. The same result is shown by the mechanical study. Thus, the addition of a high reinforcement rate (3% of KNG-180) does not seem to be a solution to have the good reinforcement–matrix adhesion. To overcome this problem, plasma treatment of GNPs was intended.

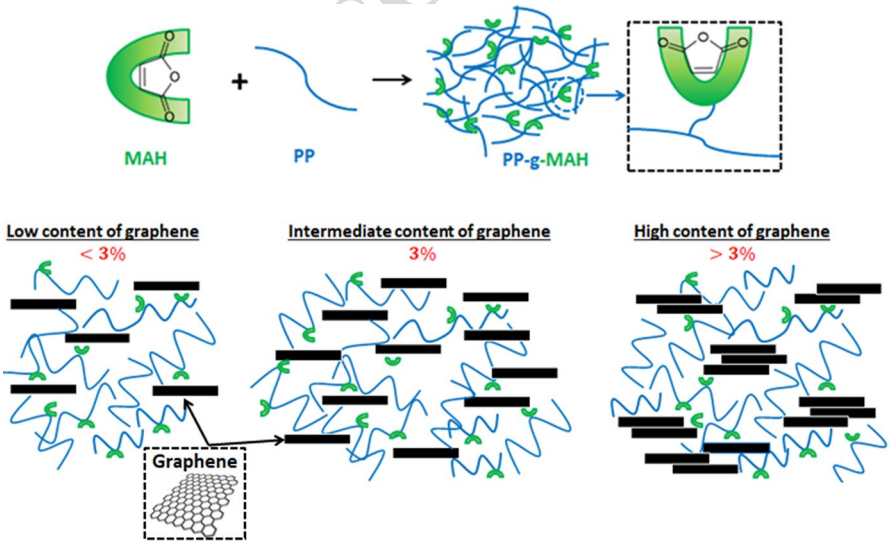

Fig. 10 Schematic illustration of GNPs/GNPs and GNPs/matrix interactions

Journal : SmallExtended 289	Article No : 4171	Pages : 20	MS Code : 4171	Dispatch : 20-3-2022

In general, oxygen plasma treatment was employed to conduct the surface functionalization of GNPs by grafting the considerable oxygen-functional groups but without noticeably damaging the structure of graphene. In [30] authors found that the plasma-treated GNPs exhibited an enhanced electrostatic affinity with Cu powder, resulting in the P-GNP/Cu composite with a uniform GNPs distribution and a good interfacial bonding. Therefore, they concluded that this treatment provides a general and effective strategy to improve graphene distribution and mechanical properties of graphene/metal composites compared with the untreated composites.

The next section describes the dielectric results obtained for plasma-treated KNG180.

Nanocomposites with plasma-treated KNG-180

Most previous studies were focused on fiber–surface treatment methods and the resultant effects on the physical, dielectric, and mechanical properties of different fiber–matrix composite systems. The improvement of dielectric properties as well as mechanical study of composites mainly depends on (i) size effect and (ii) charge distribution between the inclusions and the matrix, (iii) the large surface area of inclusions, which creates large interaction with the matrix and (iv) changing the polymer morphology due to the surface of inclusions [31]. In this section, as said before, this paper described the study of the relationship between surface modification of GNPs via plasma treatment and the GNPs/matrix interactions.

Figure 11 shows the real and imaginary parts of the complex permittivity versus frequency, for the nanocomposites KNG-180 1% with plasma-treated GNPs. Likewise, to untreated KNG-180, the dielectric analyses of treated KNG-180 shows the presence of the α_c relaxation related to the crystalline phase, the sub-glass transition relaxation (β-relaxation), the MWS interfacial polarization and the electrode polarization.

From Fig. 12, the impact of plasma treatment on the dielectric responses of the KNG-180 (from 1 to 5%) nanocomposites is manifested.

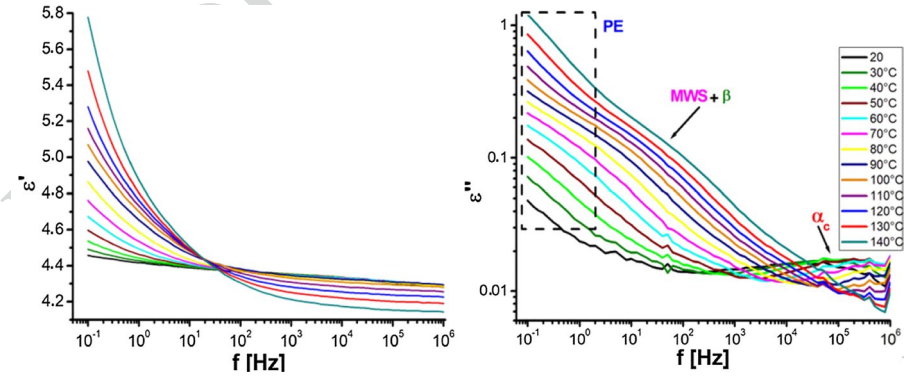

Fig. 11 Frequency dependence of ε' and ε'' for the plasma-treated nanocomposites KNG-180 1% at the temperature region [20–140 °C]

Journal : SmallExtended 289	Article No : 4171	Pages : 20	MS Code : 4171	Dispatch : 20-3-2022

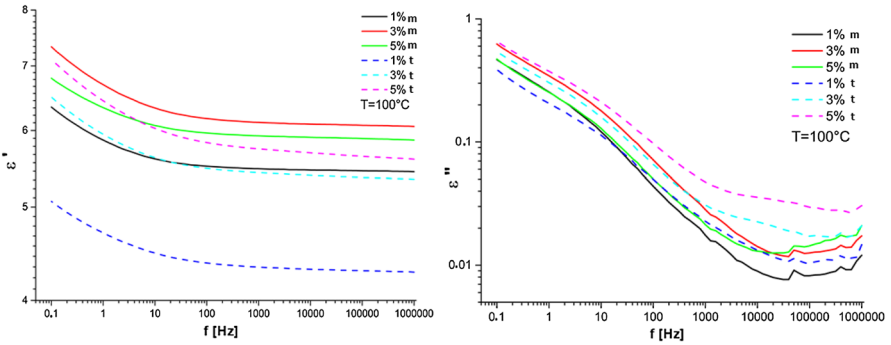

Fig. 12 Frequency dependence of ε' and ε'' for the untreated and the plasma-treated nanocomposites KNG-180 1%, KNG-180 3% and KNG-180 5% at 100 °C

As observed, an increase in ε' is much more significant for the untreated nanocomposites compared to the treated ones. It is possible to explain such behaviour by evaluating the interfacial polarization intensities $\Delta\varepsilon_{\mathrm{MWS}}$ for both untreated and treated nanocomposites (see Table 2).

Similar to untreated nanocomposites, an increase of $\Delta\varepsilon_{MWS}$ can be noted with the temperature for all the treated nanocomposites for the same reason [4, 28].

In addition, a difference in the value of $\Delta\varepsilon_{\mathrm{MWS}}$ between untreated and treated nanocomposites can be noticed. In fact, untreated nanocomposites show the highest values of $\Delta\varepsilon_{\mathrm{MWS}}$ for 1% and 3% of GNPs and the lowest values for 5% of GNPs compared to treated nanocomposites.

The plasma treatment of GNPs was performed to exfoliate, functionalized the graphite structure and have good bonding between GNP and matrix GNPs–matrix and, therefore, getting a composite with good mechanical performance. Those result found in the case of plasma treated KNG180 5% is not expected. The increase of $\Delta\varepsilon_{MWS}$ indicates not only the significant degradation of GNPs–matrix interactions, but also a significant increase in GNPs–GNPs interactions. As the obtained ATG and DRX results, as well as the SEM and TEM observations, did not show any degradation in the dispersion of GNPs between 3 and 5% of GNPs, it is more consistent to associate this evolution with the greatest interaction between GNPs. This can be explained by the fact that the plasma treatment has reduced the thickness of the GNPs, they can be distributed more evenly within the matrix, reducing the distance between the GNPs and increasing their interaction.

However, a decrease of $\Delta\varepsilon_{\mathrm{MWS}}$ is detected for the treated KNG180 1% and KNG180 3%. The plasma treatment leads to these nanocomposites showing significantly improved interfacial bonding as compared to untreated ones. Those results were in good agreement with the DMA analysis. On the contrary to Wenying Zhou et al. [32] this system is not a percolative polymer nanocomposite and this system is not concerned with intra-particle polarization but only inter-particle polarization and interaction between the macromolecular chain of the matrix and the graphite nanofillers.

Journal : SmallExtended 289	Article No : 4171	Pages : 20	MS Code : 4171	Dispatch : 20-3-2022

Table 2 MWS polarization intensities for untreated and plasma treated nanocomposites

	$\Delta\varepsilon_{\mathrm{MWS}}$ (1801*m*%)	$\Delta\varepsilon_{\mathrm{MWS}}$ (1801*t*%)	$\Delta\varepsilon_{\mathrm{MWS}}$ (1803*m*%)	$\Delta\varepsilon_{\mathrm{MWS}}$ (1803*t*%)	$\Delta\varepsilon_{\mathrm{MWS}}$ (1805*m*%)	$\Delta\varepsilon_{MWS}$ (1805*t*%)
100 °C	0.24	0.19	0.18	0.10	0.26	0.46
110 °C	0.27	0.20	0.19	0.12	0.29	0.49
120 °C	0.28	0.22	0.26	0.13	0.32	0.51
130 °C	0.35	0.29	0.34	0.15	0.39	0.39
140 °C	0.40	0.35	0.39	0.19	0.43	0.43

Journal : SmallExtended 289	Article No : 4171	Pages : 20	MS Code : 4171	Dispatch : 20-3-2022

Conclusions

In this work, a new plasma treatment [10] was used to modify a graphite nanofiller to produce two types of nanocomposites. The two fillers exhibit variations of thickness and surface functionalization as shown before. The polymer matrix used was a PP-g-MAH crosslinked with polyether amine molecules. Both nanocomposites were produced by twin-screw reactive extrusion [6]. The nanocomposite characterization exhibits important variation of the fillers dispersion inside the crosslinked polymer depending of the fillers concentration and functionalization, with a rise of the dispersion quality with the plasma treatment and the absence of aggregation at 5 wt%.

The nanocomposite characterization by DMA shows the polypropylene classic relaxational phenomena (α-, β- and γ-relaxations) but the temperature associated to those relaxations remains close for the different fillers and carbon concentrations [2, 6]. In addition, as no information can be obtained by DMA on the graphite/polymer interphase; it was thus necessary to analyze the fillers/polymer interactions with dynamical dielectric spectroscopy.

In this paper, it was shown that Dynamical dielectric spectroscopy results exhibit an additional process, the interfacial polarization known as the Maxwell–Wagner–Sillars (MWS) effect that can be used to characterize the polymer/filler interphases. The interfacial polarization increments $\Delta\epsilon_{MWS}$ calculated from the MWS relaxation can be correlated with the fillers dispersion observed by SEM and TEM microscopies. This can be used as a new way to analyse the Graphite/polymer and Graphite/graphite interaction inside the nanocomposite. The 5 wt% treated graphite nanocomposite shows an interesting evolution. This nanocomposite exhibits a good dispersion of the nano-fillers but also a high value of $\Delta\epsilon_{\mathrm{MWS}}$, which is an indication of high graphite/graphite interaction. This evolution could indicate that this material can be close to the formation of an electrical percolation network.

Acknowledgements The authors thank S. Migot and J. Ghanbaja (CC3M, Jean Lamour Institute) for TEM analysis and the collaborators C. Hérold, G. Henrion and C. Noel for the GNP plasma treatment from IJL and S. Hoppe for the reactive extrusion process from LRGP. This work was partially supported by the internal and strategical project CoPoGraF of the Jean Lamour Institute and by a MESR grant of the French government.

References

1. Wang D, Zhang X, Zha J et al (2013) Dielectric properties of reduced graphene oxide/polypropylene composites with ultralow percolation threshold. Polymer 54:1916–1922. https://doi.org/10.1016/j.polymer.2013.02.012
2. Létoffé A, García-Rodríguez SM, Hoppe S et al (2019) Switching from brittle to ductile isotactic polypropylene-g-maleic anhydride by crosslinking with capped-end polyether diamine. Polymer 164:67–78. https://doi.org/10.1016/j.polymer.2019.01.015
3. Ha C, Cho Y, Go J et al (2000) Dynamic mechanical properties of polypropylene-g-maleic anhydride and ethylene–propylene–diene terpolymer blends: effect of blend preparation methods. J Appl Polym Sci 77:2777–2784. https://doi.org/10.1002/1097-4628(20000919)77:12

Journal : SmallExtended 289	Article No : 4171	Pages : 20	MS Code : 4171	Dispatch : 20-3-2022

4. Agrebi F, Ghorbel N, Ladhar A et al (2017) Enhanced dielectric properties induced by loading cellulosic nanowhiskers in natural rubber: Modeling and analysis of electrode polarization. Mater Chem Phys 200:155–163. https://doi.org/10.1016/j.matchemphys.2017.06.058
5. Rekik H, Ghallabi Z, Royaud I et al (2013) Dielectric relaxation behaviour in semi-crystalline polyvinylidene fluoride (PVDF)/TiO2 nanocomposites. Compos Part B 45:1199–1206. https://doi.org/10.1016/j.compositesb.2012.08.002
6. Létoffé A, Hoppe S, Lainé R et al (2019) Resilience improvement of an isotactic polypropylene-g maleic anhydride by crosslinking using polyether triamine agents. Polymer 179:121655. https://doi.org/10.1016/j.polymer.2019.121655
7. Lara A, Létoffé A, Hoppe S et al (2020) Elaboration and characterization of an isotactic polypropylene-g-maleic anhydride crosslinked by a bis(amino)-calix[4]arene derivative. J Appl Polym Sci 138:49889. https://doi.org/10.1002/app.49889
8. Novais RM, Covas JA, Paiva MC (2012) The effect of flow type and chemical functionalization on the dispersion of carbon nanofiber agglomerates in polypropylene. Compos Part A 43:833–841. https://doi.org/10.1016/j.compositesa.2012.01.017
9. Butylina S, Hyvärinen M, Kärki T (2012) A study of surface changes of wood-polypropylene composites as the result of exterior weathering. Polymer Degradation stability 97:337–345. https://doi.org/10.1016/j.polymdegradstab.2011.12.014
10. Jeffamines® Polyetheramines, Technical Specifications Sheet by Hunstman.
11. Létoffé A, Cuynet S, Noel C et al (2021) Functionalisation and exfoliation of a nano-graphite with low temperature pulse plasma in distilled water. Phys Chem Chem Phys (**submitted, under review**) AQ2
12. Ozkazanc E, Zor S, Ozkazanc H et al (2012) Synthesis, characterization and dielectric behavior of (ES)-form polyaniline/cerium(III)-nitrate-hexahydrate composites. Mater Chem Phys 133:356–362. https://doi.org/10.1016/j.matchemphys.2012.01.037
13. Sarkar A, Ghosh P, Meikap AK et al (2008) Electrical-transport properties of iodine-doped conducting polyaniline. J Appl Polym Sci 108:2312. https://doi.org/10.1002/app.27615
14. Qi YN, Xu F, Ma HJ et al (2008) Thermal stability and glass transition behavior of PANI/MWNT composites. J Therm Anal Calorim 91:219. https://doi.org/10.1007/s10973-008-8978-2
15. Arous M, Ben Amor I, Boufi S et al (2007) Experimental study on dielectric relaxation in alfa fiber reinforced epoxy composites. J Appl Polym Sci 106:3631–3640. https://doi.org/10.1002/app.26885
16. Ladhar A, Arous M, Kaddami H et al (2014) Molecular dynamics of nanocomposites natural rubber/cellulose nanowhiskers investigated by impedance spectroscopy. J Mol Liq 196:187–191. https://doi.org/10.1016/j.molliq.2014.03.040
17. Addiego F, Dahoun A, G'Sell C et al (2006) Characterization of volume strain at large deformation under uniaxial tension in high-density polyethylene. Polymer 47:4387–4399. https://doi.org/10.1016/j.polymer.2006.03.093
18. Potts JR, Dreyer DR, Bielawski CW et al (2011) Graphene-based polymer nanocomposites. Polymer 52:5–25. https://doi.org/10.1016/j.polymer.2010.11.042
19. Gulrez SKH, Mohsin MEA, Shaikh H et al (2013) A review on electrically conductive polypropylene and polyethylene. Polym Compos 35:900–914. https://doi.org/10.1002/pc.22734
20. Havriliak S, Negami S (1966) A complex plane analysis of a-dispersions in some polymer systems. J Polym Sci Part C 14:99–117. https://doi.org/10.1002/polc.5070140111
21. Havriliak S, Negami S (1967) A complex plane representation of dielectric and mechanical relaxation processes in some polymers. Polymer 8:161–210. https://doi.org/10.1016/0032-3861(67)90021-3
22. Ridhore A, Jog JP (2012) A dynamic mechanical and dielectric relaxation study of PP-g-MAH/ clay nanocomposites. Open Macromol J 6:53–58. https://doi.org/10.2174/1874343901206010053
23. Bettini SHP, Agnelli JAM (2002) Grafting of maleic anhydride onto polypropylene by reactive extrusion. J Appl Polym Sci 85:2706–2717. https://doi.org/10.1002/app.10705
24. Motori A, Montanari G, Saccani A et al (2007) Electrical conductivity and polarization processes in nanocomposites based on isotactic polypropylene and modified synthetic clay. J Polym Sci Part B Polym Phys 45:705–713. https://doi.org/10.1002/polb.21091
25. Bohning M, Goering H, Fritz A et al (2005) Dielectric study of molecular mobility in poly (propylene-graft-maleic anhydride)/clay nanocomposites. Macromolecules 38:2764–2774. https://doi.org/10.1021/ma048315c
26. Jin X, Zhang S, Runt J (2002) Observation of a fast dielectric relaxation in, semicrystalline poly(ethylene oxide). Polymer 43:6247–6254. https://doi.org/10.1016/S0032-3861(02)00560-8

Journal : SmallExtended 289	Article No : 4171	Pages : 20	MS Code : 4171	Dispatch : 20-3-2022

27. Havriliak S, Havriliak SJ (1996) Comparaison of the Havriliak-Negami and stretched exponential functions. Polymer 37:4107–4110. https://doi.org/10.1016/0032-3861(96)00274-1
28. Triki A, Guicha M, Ben Hassen M et al (2011) Studies of dielectric relaxation in natural fibres reinforced unsaturated polyester. J Mater Sci 46:3698–3707. https://doi.org/10.1007/s10853-010-5136-6
29. Ladhar A, Arous M, Kaddami H et al (2017) Correlation between the dielectric and the mechanical behavior of cellulose nanocomposites extracted from the rachis of the date palm tree. In: Paper presented at the IOP conference series: materials science and engineering, vol 258, pp 012001. https://doi.org/10.1088/1757-899X/258/1/012001
30. Chu K, Liu Y, Wang J et al (2018) Oxygen plasma treatment for improving graphene distribution and mechanical properties of graphene/copper composites. Mater Sci Eng A 735:398–407. https://doi.org/10.1016/j.msea.2018.08.064
31. Mittal V (2016) Spherical and fibrous filler composites. Wiley, New York, p 8. https://doi.org/10.1002/9783527670222
32. Zhou W, Li T, Yuan M, Li Bo, Dang Z-M (2021) Decoupling of inter-particle polarization and intra-particle polarization in core-shell structured nanocomposites towards improved dielectric performance. Energy Storage Mater 42:1–11. https://doi.org/10.1016/j.ensm.2021.07.014

Journal:	**289**
Article:	**4171**

Author Query Form

Please ensure you fill out your response to the queries raised below and return this form along with your corrections

Dear Author

During the process of typesetting your article, the following queries have arisen. Please check your typeset proof carefully against the queries listed below and mark the necessary changes either directly on the proof/online grid or in the 'Author's response' area provided below

Query	Details Required	Author's Response
AQ1	Author details: Kindly check and confirm whether the corresponding author affiliation is correctly identified.	
AQ2	Please update Ref. [11] with volume id and page range, if possible.	